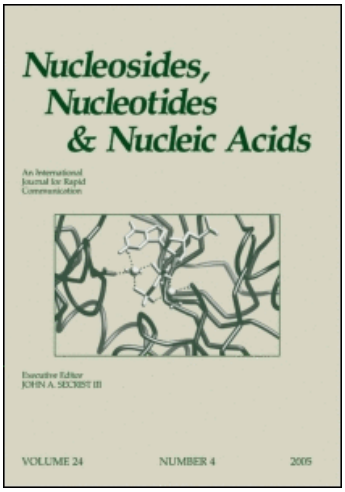

Nucleosides, Nucleotides and Nucleic Acids
Publication details, including instructions for authors and subscription information:
http://www.informaworld.com/smpp/title~content=t713597286

BINDING OF A PORPHYRIN CONJUGATE OF HOECHST 33258 TO DNA. I. UV-VISIBLE AND MELTING STUDIES DETECT MULTIPLE BINDING MODES TO A 12-MER NONSELF-COMPLEMENTARY DUPLEX

Silvana Frau[a]; Elena V. Bichenkova[a]; Olga S. Fedorova[b]; Serghei Lokhov[b]; Kenneth T. Douglas[a]
[a] School of Pharmacy and Pharmaceutical Sciences, University of Manchester, Manchester, U.K. [b] Institute of Bioorganic Chemistry, Novosibirsk, Russia

Online publication date: 26 February 2001

To cite this Article Frau, Silvana , Bichenkova, Elena V. , Fedorova, Olga S. , Lokhov, Serghei and Douglas, Kenneth T.(2001) 'BINDING OF A PORPHYRIN CONJUGATE OF HOECHST 33258 TO DNA. I. UV-VISIBLE AND MELTING STUDIES DETECT MULTIPLE BINDING MODES TO A 12-MER NONSELF-COMPLEMENTARY DUPLEX', Nucleosides, Nucleotides and Nucleic Acids, 20: 1, 131 — 143
To link to this Article: DOI: 10.1081/NCN-100001442
URL: http://dx.doi.org/10.1081/NCN-100001442

NUCLEOSIDES, NUCLEOTIDES & NUCLEIC ACIDS, 20(1&2), 131–143 (2001)

BINDING OF A PORPHYRIN CONJUGATE OF HOECHST 33258 TO DNA. I. UV-VISIBLE AND MELTING STUDIES DETECT MULTIPLE BINDING MODES TO A 12-MER NONSELF-COMPLEMENTARY DUPLEX

Silvana Frau,[1] Elena V. Bichenkova,[1] Olga S. Fedorova,[2] Serghei Lokhov,[2] and Kenneth T. Douglas[1,*]

[1]School of Pharmacy and Pharmaceutical Sciences, University of Manchester, Manchester M13 9PL, U.K.
[2]Institute of Bioorganic Chemistry, 8 Lavrentyev Avenue, 630090, Novosibirsk, Russia

ABSTRACT

Relative to ligand-free duplex DNA, the melting temperature of the 1:1 complex of the duplex d(CGAATTGTATGC):d(GCATACAATTCG) with the conjugate of Hoechst 33258 with a *des*-metalloporphyrin, increased from 42 to 60.5°C indicating strong ligand binding. UV–vis spectrophotometric titration detected more than one class of binding site (apparent dissociation constants $\sim 0.2\ \mu M$ for simple noncooperative binding and $1\ \mu M$ for the simultaneous cooperative mode with Hill coefficient ~ 2).

Key Words: DNA binding; Minor groove; Single strand DNA ligand; Chemical nucleases.

INTRODUCTION

The minor groove of DNA has been discussed as a target for the design of drugs and the fluorescent dye Hoechst 33258 (HOE) is now well established as

*Address correspondence to K. T. Douglas. E-mail: Ken.Douglas@man.ac.uk

a model for minor groove ligand design (1–4), binding strongly and selectively to double-stranded B-DNA A−T tracks. Metal free and four-coordinate cationic porphyrins, such as tetrakis (4-*N*-methylpyridiniumyl) porphyrin (H_2T_4MPyP) and Cu(II)T4MpyP, interact with DNA preferentially in GC regions (unlike the Zn(II), Fe(III), Mn(III), and Co(III) derivatives) by true or hemi intercalation (5–7). In AT regions, porphyrin binding appears to be external and coulombic, possibly involving the minor groove (8). Footprinting (9,10) and NMR (11) studies have implicated both CpG and TpA as preferred targets.

A chemical nuclease conjugating a tris (4-*N*-methylpyridiniumyl) Mn(III) porphyrin motif to Hoechst 33258 causes cleavage/damage to two different areas of selected 35-mer ds oligonucleotide (12,13). This could indicate two possible orientations of the molecule with respect to the cleavage sites, or there may be a sequence-induced configurational effect on the local minor groove, creating "hot sites" with respect to cleavage susceptibility. We report results of a study of the interaction between the nonmetallated porphyrin conjugate molecule H_2TrisMPyP-Hoechst 33258 (PORHOE, Scheme 1) and a non-self-complementary, 12-mer double-stranded (ds) oligonucleotide, using melting temperature analysis and UV–vis spectrophotometry. This 12-mer oligonucleotide was designed to contain the affinity sites of both Hoechst 33258 (5′-AATT-3′) and MnTMPyP (5′-TAT-3′) based on the nuclease experiments for the 35-mer (13). Because of the paramagnetism of the Mn(III) nucleus, we first studied the interaction of the nonmetallated derivative with the oligonucleotide as a basis for NMR analysis (see Part II).

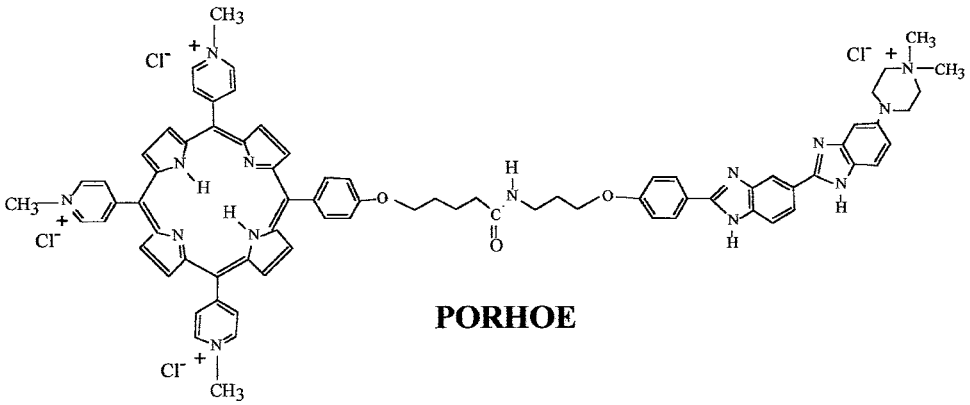

PORHOE

5' 1C 2G 3A 4A 5T 6T 7G 8T 9A 10T 11G 12C 3'

3' 24G 23C 22T 21T 20A 19A 18C 17A 16T 15A 14C 13G 5'

Scheme 1.

MARCEL DEKKER, INC.
270 Madison Avenue, New York, New York 10016

MATERIALS AND METHODS

The conjugate porphyrin–Hoechst 33258 (PORHOE) was synthesized and characterized as previously reported (14,15). Hoechst 33258 and 5, 10, 15 20-tetrakis(1-methyl-4-pyridyl)-21H,23H-porphyrin tetra-*p*-tosylate (POR) were from Aldrich Chemical Co.

UV–vis spectra were measured on a Cary-Varian 1E [operating system/2 (version 3) and the CARY 1 software] at various temperatures. Spectrophotometric analysis of binding between 12-mer duplex and PORHOE, Hoechst 33258 or POR was performed in buffer A (10 m*M* NaH_2PO_4/Na_2HPO_4, pH 7.0, 100 m*M* NaCl, 0.1 m*M* EDTA). In the case of Hoechst 33258–12-mer and POR–12-mer complexes the binding analysis was carried out at 25°C with equimolar ligand and duplex (2 μM). The binding between PORHOE and duplex was analyzed at 20, 60, and 100°C with equimolar (5 μM) ligand and duplex. After complex formation, the sample was allowed to equilibrate thermally for 10 min. Binding isotherms for 12-mer–PORHOE complex formation were obtained by spectrophotometric titration of 1.65 μM PORHOE in buffer A at 20°C with increasing amounts of the duplex d(CGAATTGTATGC):d(GCATACAATTCG), monitored at 437 and 342 nm.

Optical melting curves were obtained using a Cary-Varian 1E UV–vis spectrophotometer (for free 12-mer duplex, 12-mer–PORHOE complex, 12-mer–porphyrin complex, and 12-mer–Hoechst 33258 complex). The experiments were performed in buffer A with a duplex concentration of 5 μM (and 4 μM). UV detection at 260 nm was used to monitor the thermal denaturation of the oligonucleotide part of the complexes. In the case of 12-mer–PORHOE complexes (5 μM) additional experiments were performed at 340 and 350 nm (for tracking the Hoechst 33258 chromophore in its unbound and bound forms, respectively), and at 430 and 437 nm (for monitoring the porphyrin chromophore in its bound and unbound environments, respectively).

RESULTS

UV–vis Spectrophotometry

In Figure 1A are shown the spectra of PORHOE free in solution (at 20°C), and as its 1:1 mixture with d(CGAATTGTATGC):d(GCATACAATTCG) in buffer A at 20, 60, and 100°C. Equimolar concentrations (5 μM) of PORHOE and oligonucleotide duplex were used. Figure 1B shows the expanded regions of these spectra (at 20, 60, and 100°C) corresponding to the Hoechst 33258-like and porphyrin chromophore absorption bands in their complexed state. In a separate run, spectra at 20 and 70°C were measured and that for the PORHOE–oligo complex on cooling back to 20°C was shown to be superimposable on the 20°C spectrum prior to heating, showing full reversibility.

From Figure 1 and Table 1, complex formation between PORHOE and 12-mer duplex shifts λ_{max} both for the Hoechst 33258 moiety (from 343 to 353 nm) and

MARCEL DEKKER, INC.
270 Madison Avenue, New York, New York 10016

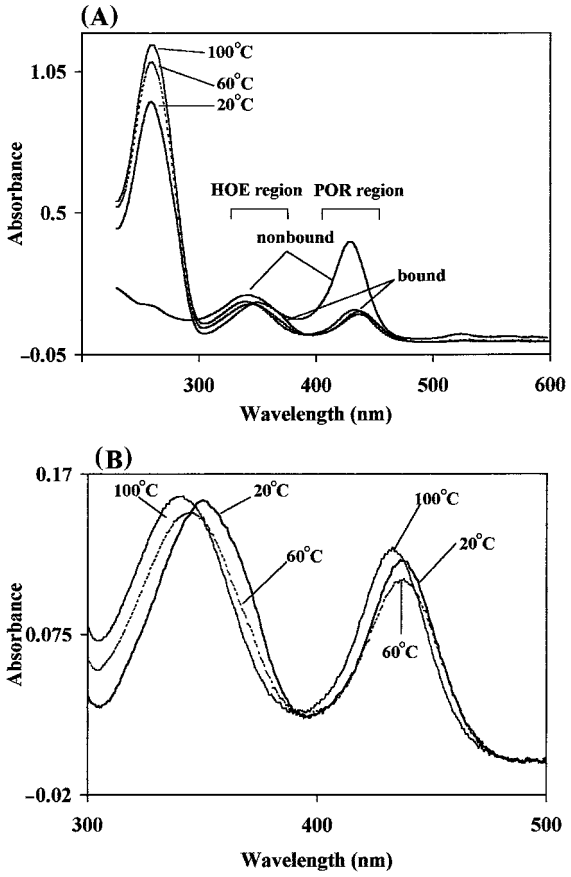

Figure 1. A) UV–vis spectra of PORHOE, both free and bound to the 12-mer duplex of d(CGAATTGTATGC):d(GCATACAATTCG) at the temperatures indicated in 10 m*M* sodium phosphate buffer pH 7.00, containing 100 m*M* NaCl and 0.1 m*M* EDTA. Equimolar (5 μM) concentrations of PORHOE and duplex were used. B) Expanded regions of spectra from (A), corresponding to the bis-benzimidazole and porphyrin chromophores of the 1:1 complex at 20, 60, and 100°C.

the porphyrin part (from 432 to 437 nm), with hypochromic effects of 15 and 69%, respectively. A similar red shift of λ_{max} was observed for free Hoechst 33258 ($\Delta\lambda_{max} = 13$ nm) and for free porphyrin POR ($\Delta\lambda_{max} = 6$ nm) on binding to the 12-mer duplex (Fig. 2A and B, respectively, and Tab. 1). However, there was a significantly smaller hypochromic effect (8.4%) for POR binding to DNA, and a slight hyperchromic effect (~2%) in the case of Hoechst 33258 binding to the same duplex. These observations are similar to those reported for external porphyrin binding to poly(dG−dC) and calf thymus DNA (16). These data may indicate that the porphyrin of PORHOE interacts more strongly with DNA than does free POR, probably due to the additional Hoechst 33258–DNA interaction.

The addition of NaCl (to 2 *M* final concentration) released POR from the duplex–POR complex, confirmed by shift of the porphyrin λ_{max} back to 424 nm

MARCEL DEKKER, INC.
270 Madison Avenue, New York, New York 10016

Table 1. UV–vis Study of Interactions Between PORHOE, POR and Hoechst 33258 (HOE) and Double-Stranded d(CGAATTGTATGC):d(GCATACAATTCG) at 25°C in pH 7.00 Buffer (10 m*M* NaH_2PO_4/Na_2HPO_4, 100 m*M* NaCl, 0.1 m*M* EDTA in H_2O)

System	λ_{max} (nm)	ε_{max} (M^{-1} cm^{-1})	ε_{max} change (%)	Literature Data ε_{max} (M^{-1} cm^{-1})	Literature Data λ_{max}(nm)
HOE in buffer (free)	340	38,450		42,000[a,b]	338[a,b]
				39,200[c]	340[c]
HOE + DUPLEX (1:1), buffer	352.5	39,050	−1.6		
HOE + DUPLEX, buffer + 1 *M* NaCl	352.5	43,000		–	360[c]
HOE + 1 *M* NaCl	343.9	22,100			
POR in buffer (free)	422.4	70,450		194,000[d]	424[d]
				206,000[e]	424[e]
POR + DUPLEX in buffer	428.2	64,650	−8.4		428[d]
POR + DUPLEX, buffer + 2 *M* NaCl	424.5	75,350			
POR + 1 *M* NaCl	423	75,000		21,500[e]	424[e]
PORHOE (free)	432	80,600			
	343	48,450			
PORHOE + DUPLEX	437	66,000	−18		
	353	40,550	−16.3		
PORHOE + DUPLEX + 1 *M* NaCl	436	75,000			
	352	48,000	−0.93		
PORHOE + 2 *M* NaCl	432.5	58,500			
	344	40,000	−17.4		

[a]Loontiens, F.G.; Regenfuss, P.; Zechal, A.; Dumortier, L.; Clegg, R.M. Biochemistry **1990**, *29*, 9029–39.
[b]Loontiens, F.G.; McLaughlin, L.W.; Diekmann, S.; Clegg, R.M. Biochemistry **1991**, *30*, 182–89.
[c]Bontemps, J.; Houssier, C.; Fredericq, E. Nucl. Acids Res. **1975**, *2*, 971–84.
[d]Fiel, R.J.; Howard, J.C.; Mark, E.H.; Datta Gupta, N. Nucl. Acids Res. **1979**, *6*, 3093–118.
[e]Carvlin, M.J.; Mark, E.; Fiel, R.; Howard, J.C. Nucl. Acids Res. **1983**, *11*, 6141–154.

and by complete recovery of the intensity of this absorbance (Fig. 2B). These data suggest a predominantly electrostatic nature for a porphyrin interaction with the outside of the DNA. In contrast, the binding of both Hoechst 33258 and the Hoechst 33258-moiety of PORHOE to the duplex was salt-independent (Tab. 1, Fig. 2A): λ_{max} values for Hoechst 33258 and for Hoechst 33258-parts of PORHOE were unaffected by salt addition. In the presence of 2 *M* NaCl, Hoechst 33258 in its bound state displays a higher hyperchromic effect (∼10%) than in low-salt conditions, indicating lower availability to the solvent. In contrast, the Hoechst 33258-part of PORHOE displays a hypochromic effect in high-salt conditions, indicating greater accessibility to solvent whilst in the 12-mer–PORHOE complex. These data provide indirect evidence for weaker interaction of the Hoechst 33258-part of PORHOE with dsDNA, compared with the Hoechst 33258–DNA interaction.

Temperature increase (to 100°C) induced thermal denaturation of the duplex (with a 25% temperature-induced hyperchromic effect at 260 nm) accompanied by

MARCEL DEKKER, INC.
270 Madison Avenue, New York, New York 10016

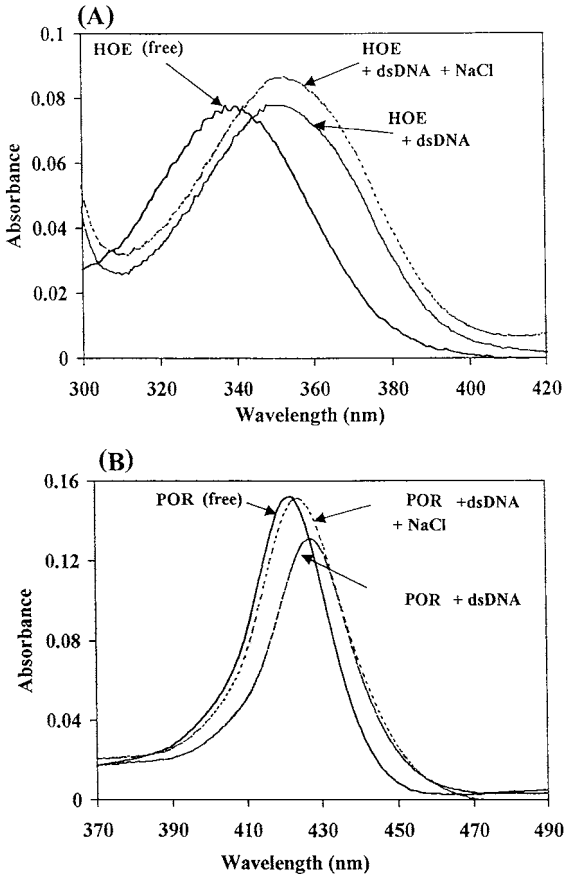

Figure 2. UV–vis spectra of A) Hoechst 33258 and B) POR, both free and bound to the 12-mer duplex of d(CGAATTGTATGC):d(GCATACAATTCG) at 25°C in 10 m*M* sodium phosphate buffer pH 7.00, containing 100 m*M* NaCl and 0.1 m*M* EDTA. Equimolar (2 μM) concentrations of respective ligand and duplex were used.

release of PORHOE from the ds helix, indicated by shifts of λ_{max} back to 343 nm for the Hoechst 33258 part and to 432 nm for POR part of the ligand (Fig. 1). Nevertheless, the absorbance at λ_{max} for neither absorbance band recovered to its respective magnitude as compared to PORHOE in the unbound state: at 100°C the hypochromic effect was 14% for the Hoechst 33258 part and 66% for the POR part, relative to free PORHOE. These data suggest a strong interaction between PORHOE and single-stranded oligonucleotide chains.

DNA Melting Data for Duplex

Figure 3A shows the melting curves at 260 nm for free duplex (curve 1), 12-mer–PORHOE complex (1:1) (curve 2), 12-mer–porphyrin complex (1:1) (curve 3), and 12-mer–Hoechst 33258 complex (1:1) (curve 4). The free duplex showed a

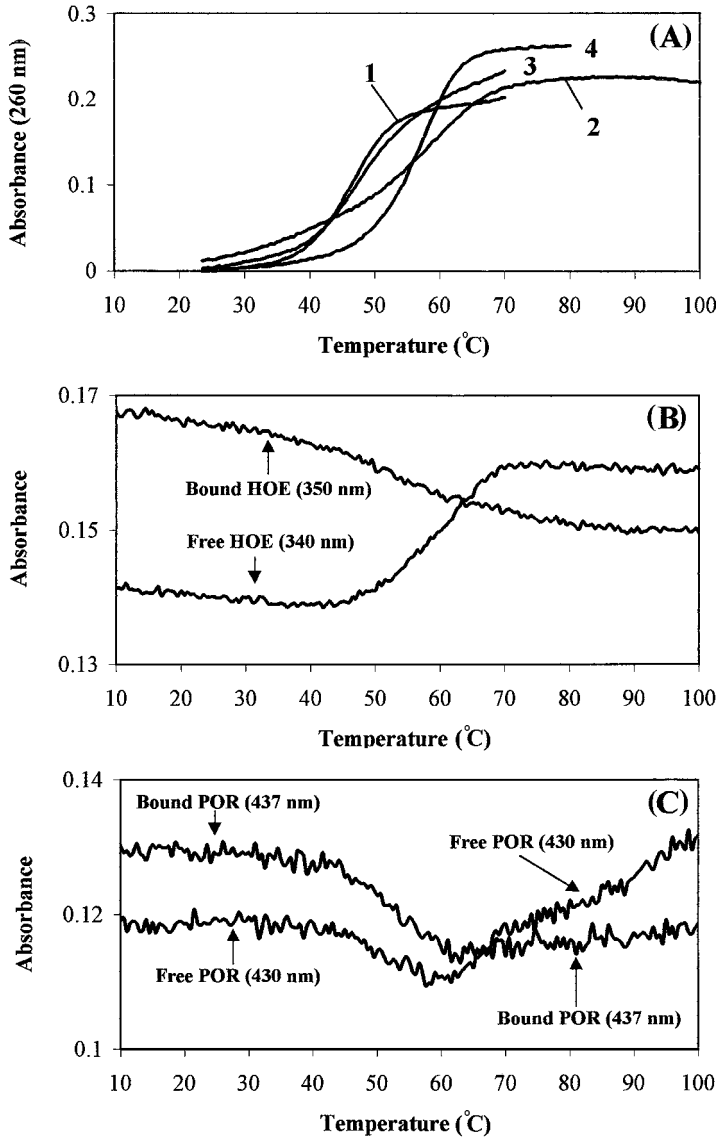

Figure 3. A) Melting profiles ($\lambda_{detection} = 260$ nm) for the free 12-mer duplex d(CGAATTGTATGC):d(GCATACAATTCG) in the absence of ligand (curve 1) and for the 1:1 complexes of 12-mer duplex with PORHOE, POR, and Hoechst 33258, respectively (curves 2, 3, and 4, respectively). In all cases oligonucleotide and ligand concentrations were 4 μM. Data obtained in 10 mM sodium phosphate buffer pH 7.00, containing 100 mM NaCl and 0.1 mM EDTA ligand. B) Melting profile for a 5 μM solution of 1:1 complex of PORHOE with d(CGAATTGTATGC):d(GCATACAATTCG) in 10 mM sodium phosphate buffer pH 7.00, containing 100 mM NaCl and 0.1 mM EDTA, followed at 340 and 350 nm to monitor changes in the Hoechst 33258-like region of the molecule. C) Melting profile for a 5μM solution of 1:1 complex of PORHOE with d(CGAATTGTATGC):d(GCATACAATTCG) in 10 mM sodium phosphate buffer pH 7.00, containing 100 mM NaCl and 0.1 mM EDTA followed at 430 and 437 nm to monitor changes in the porphyrin region of the molecule.

MARCEL DEKKER, INC.
270 Madison Avenue, New York, New York 10016

well-behaved cooperative melting transition with $T_m = 45°C$ (curve 1). The half-transition for 12-mer–PORHOE complex at 260 nm showed $T_m = 60.5°C$ with a distorted sigmoid profile (Fig. 3A), denaturation proceeding over a very broadened temperature interval. Thus, the 2-state model is not applicable for the PORHOE–12-mer complex.

The melting profiles obtained at 340 and 350 nm (Fig. 3B) clearly show the dissociation of the Hoechst 33258-moiety of PORHOE from a minor groove DNA complex. This behavior is typical of the melting profiles of minor groove binders monitored through λ_{max} of the chromophore rather than using the A_{260} profile of the DNA base pairs, and has been analysed fully by both UV–vis spectrophotometry and high-field NMR/distance geometry calculation for a pyrene-binding system (17). Figure 3B shows that the absorbance increases with temperature at 340 nm (free ligand) and decreases at 350 nm (bound ligand). The T_m obtained at 340 nm was 58°C, indicating release of the Hoechst 33258-moiety of PORHOE from the minor groove slightly earlier than duplex dissociation.

The behavior of ligand as monitored by means of the porphyrin moiety (Fig. 3C) is more complex. Following the melting profiles at 437 nm (bound ligand), straightforward ligand dissociation appears to occur ($T_m \sim 53°C$). However, the 430 nm data show that even at 100°C the porphyrin is still not in the fully free state, as the A_{430} increases steadily from 60 to 100°C with no evidence of a plateau being reached. These data are in agreement with spectra of the 12-mer–PORHOE complex at 100°C (Fig. 1) showing that neither the Hoechst 33258 nor the POR part recovered absorbance at their respective λ_{max} values after complete duplex dissociation. From 40 to 60°C, the A_{430} decreases with temperature, presumably signalling a duplex rearrangement. Based on these data, it is reasonable to propose that when the duplex starts to melt, the porphyrin part of the PORHOE continues to interact with the single-stranded oligos even at the high temperatures.

We investigated the stabilization effects originating from separate components of PORHOE (i.e., POR–12-mer and Hoechst 33258–12-mer interactions), using melting experiments at 260 nm (Fig. 3A). Table 2 presents the T_m values for 12-mer duplex alone, 12-mer duplex with PORHOE, 12-mer duplex with POR, and 12-mer duplex with Hoechst 33258, all obtained under similar conditions (4 μM duplex concentration, buffer A). The stabilization effect of Hoechst 33258 on the 12-mer duplex is significantly greater ($\Delta T_m = 12.5°C$) than that of just POR ($\Delta T_m = 3.5°C$). The stabilization effect of PORHOE ($\Delta T_m = 15.5°C$) arises mostly from the Hoechst 33258-moiety, with a small, additive contribution from the POR part.

Spectrophotometric Titration of the Duplex with PORHOE

The binding isotherm for PORHOE with the duplex (Fig. 4) is complex and shows at least two binding modes, as there is a maximum in the change in absorbance

MARCEL DEKKER, INC.
270 Madison Avenue, New York, New York 10016

Table 2. Melting Temperature Data for Free 12-mer Duplex, d(CGAATTGTATGC):d(GCATACAATTCG), and its Complexes with PORHOE, POR, and Hoechst 33258 (HOE) Monitored at Various Wavelengths[a]

DUPLEX	$\lambda_{detection}$ (nm)	Concentration	T_m	ΔT_m
Free DUPLEX	260	4.0 μM	45°C	
DUPLEX + PORHOE (Oligo bp monitored)	260	4.0 μM	60.5°C	15.5°C
DUPLEX + PORHOE (HOE part monitored)	340	5.0 μM	58°C	
DUPLEX + PORHOE (POR part monitored)	437	5.0 μM	~53°C	
DUPLEX + HOE	260	4 μM	57.5°C	12.5°C
DUPLEX + POR	260	4 μM	48.5°C	3.5°C

[a]All thermal denaturation experiments were performed in 100 mM NaCl, 10 mM $NaH_2/PO_4/Na_2HPO_4$, pH 7.00, 0.1 mM EDTA buffer.

at either 342 or 437 nm. The data are shown with a curve fitted corresponding to Equation (1):

$$Y = [C[\text{oligo}]/(\text{Ka} + [\text{oligo}]) + C'[\text{oligo}]^n/(\text{Kb} + [\text{oligo}]^n)] \quad (1)$$

The values of the parameters obtained by nonlinear regression analysis of the data at 342 nm are as follows (with the corresponding fitted value for 437 nm in parentheses): C, 0.04 (0.09); Ka, 0.23 μM (0.22 μM); C', −0.02 (−0.05); n, 2.0 (1.7); Kb, 1.09 μM (1.01 μM). We do not regard these extracted parameters as highly dependable as the fitting is sensitive to the initial estimates, the most useful value of the lines generated for Figure 4 is to aid visualization. The McGhee–Von Hippel model applied to these data would have seven unknowns and be

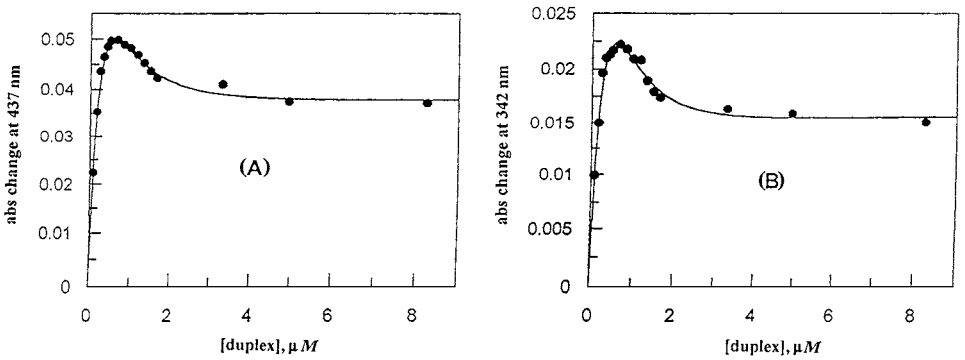

Figure 4. Binding isotherms from spectrophotometric titration of 1.65 μM PORHOE in 10 mM sodium phosphate buffer at pH 7.00 containing 100 mM NaCl and 0.1 mM EDTA at 20°C with increasing amounts of the duplex of d(CGAATTGTATGC):d(GCATACAATTCG), monitored at A) 437 nm and B) 342 nm. Points are experimental: line is derived from Equation (1) as described in the text.

statistically incorrect to fit using the limited data available here for any single curve. The extended McGhee–Von Hippel model dealing with binding in two or more noninterfering ways proliferates unknown parameters at a rate greater than can be handled experimentally (18).

DISCUSSION

The UV–vis spectrum of the PORHOE conjugate is strongly perturbed by binding to duplex d(CGAATTGTATGC):d(GCATACAATTCG). The λ_{max} of the Hoechst 33258 moiety shifts from 340 to 350 nm, characteristic of the minor groove binding of Hoechst 33258 and analogues to duplex DNA, which has been confirmed and analysed in great detail by high resolution structural techniques (4,19–22). The Soret band of the POR group shifts from 430 to 437 nm with very strong hypochromicity (∼three-fold), characteristic of *des*-metallocationic porphyrin binding to duplex DNA (23,24).

The T_m of the 12-mer duplex was increased from 45 to 60.5°C by the addition of equimolar amount of PORHOE, providing evidence for tight binding and strong stabilization by the ligand. For Hoechst 33258 and meta-Hoechst (the meta-hydroxy isomer of Hoechst 33258) binding to calf-thymus DNA, the change in T_m was 8–10°C, but for poly(dA).poly(dT) it was over 30°C (2).

Feng et al. report binding constants of $0.5–0.9 \times 10^5\ M^{-1}$ with calf thymus DNA (25) for the initial outside binding of the first H2TMPyP-4 molecule prior to interaction caused by subsequent ligand site occupancy. Metal-free H2TMPyP-4 has been established by to intercalate selectively at GC-rich regions (especially CpG) of duplex DNA (26). Binding constants for the poly d(G−C):poly d(G−C) duplex with metal-free cationic porphyrins are $\sim 7 \times 10^5\ M^{-1}$ (5,28,29). For cationic porphyrins with a range of side chains, association constants for binding to calf thymus DNA were in the range $10^6–10^7\ M^{-1}$, according to the McGhee–Von Hippel model (18).

The spectrophotometric titration of PORHOE with duplex (Fig. 4) is complex to extract meaningful dissociation constants from, but may minimally be explained by two essentially independent binding processes, a simple noncooperative process with an apparent dissociation constant for the complex of $\sim 0.2\ \mu M$ and a cooperative binding mode with apparent dissociation constant $\sim 1\ \mu M$ and a Hill coefficient of ∼2.

The melting profile of the complex monitored through the DNA base-pairs (Fig. 3A) or Hoechst 33258 moiety region (Fig. 3B) of the ligand chromophore appeared to give reasonably straightforward cooperative melting. At higher temperatures, the Hoechst 33258 part of the chromophore moved from a bound to an unbound environment, and at temperatures above 90°C the 350 nm wavelength transition and spectra are consistent with the ligand being in essentially free solution. However, monitoring the porphyrin moiety with increasing temperature indicates that, in spite of some conformational changes observed for porphyrin in temperature

MARCEL DEKKER, INC.
270 Madison Avenue, New York, New York 10016

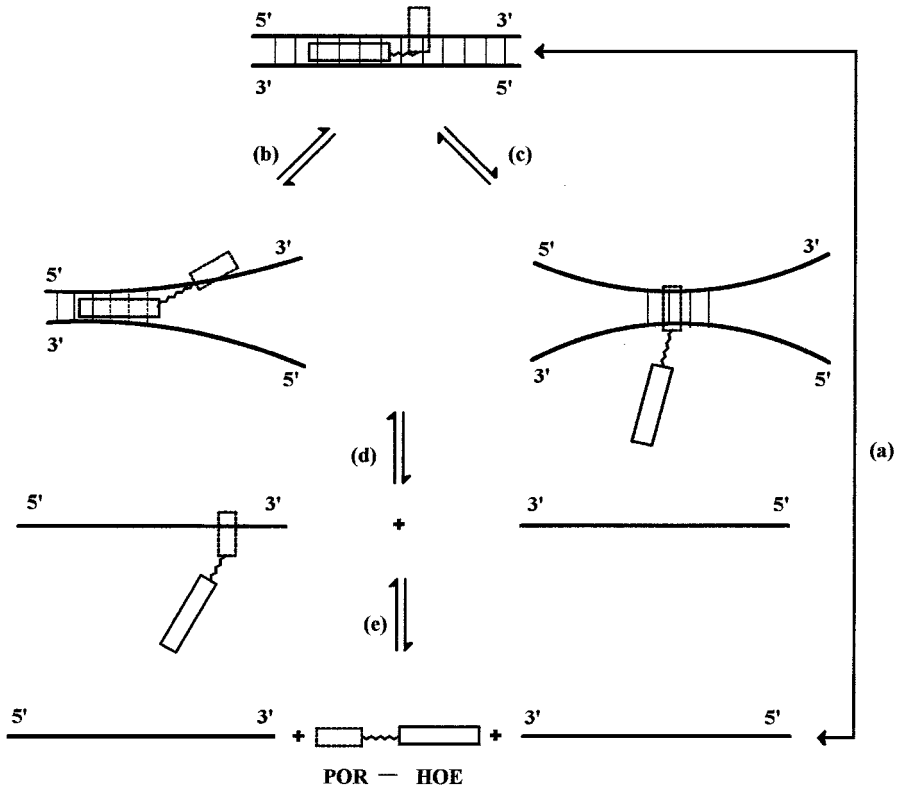

Scheme 2. Model for the sequence of melting events for the complex between PORHOE and d(CGAATTGTATGC):d(GCATACAATTCG). At low temperature a 1:1 complex is formed, which on complete melting forms separate single strands and ligand in process (a). Processes (b) and (c) represent local dissociation of (b) the porphyrin end of PORHOE in preference to the Hoechst 33258 region and (c) the reverse situation. As temperature increases further (process (d)), complete strand separation occurs, but the ligand can remain associated with either of the single strands (only one shown). Eventually the ligand, single strand complex dissociates with increased temperature (process (e)).

interval between 45 and 60°C (Fig. 3C), even at 100°C the porphyrin chromophore is not in a bulk solution environment (consider the A_{430} profile for "free" porphyrin). Scheme 2 shows the situation diagrammatically. At temperatures around 60°C, DNA melting occurs and strand-separation ensues. This enforces complex dissociation, which can be of a) the complete ligand release (the 2-state model); b) the release of the porphyrin end of PORHOE first; and/or c) the release of the Hoechst 33258 end of PORHOE first. In reality there is likely to be a continuum of events between extrema (b) and (c). The T_m for complex transition obtained by monitoring at 260 nm (oligonucleotide part) is 60.5°C. The corresponding value evaluated by registration at 340 nm (Hoechst moiety) is 58°C, indicating that release of the Hoechst 33258-moiety of PORHOE from the minor groove occurs slightly earlier than complete duplex dissociation. Following the porphyrin moiety as an indicator shows apparent T_m values (estimated as the temperature of inflexion) of

53 and 54°C at 430 and 437 nm, respectively. This indicates that the conformational rearrangement of porphyrin starts before total separation of oligonucleotide chains and release of the Hoechst 33258-moiety from the complex. The data on T_m, obtained for the Hoechst-part and porphyrin moiety, are in accord with the known binding constants of Hoechst 33258 for duplex oligonucleotides, which are reported as $\sim 10^9$ *M* for d(CGCGAATTCGCG)$_2$ (21) and 10^6 *M* for *des*-metallocationic porphyrins (16,23,27), a difference in binding energy of approximately 5 kcal mol^{-1} (using $\Delta\Delta G = 2.303RT\,\Delta pK^{ass}$).

The structural rearrangement found for the porphyrin moiety in the temperature interval from 40 to 60°C seems to be associated with the decrease of porphyrin contacts with the duplex accompanying the increase of its interactions with the single ssDNA chains (without competition from the complementary oligo strand). This model explains the experimental observations on the unusual decrease in intensity for the 430 nm band (corresponding to nonbound porphyrin) observed in the temperature interval from 40 to 60°C (Fig. 3C), and the failure of complete recovery in intensity for the porphyrin moiety, even after total duplex dissociation at 100°C (Fig. 1A). The A_{430} of a fully free porphyrin is ~3 times as intense as the observed value for the PORHOE–oligo system heated to 100°C. Thus, it is clear that the porphyrin is still associated with the ssDNA in some way (an aspect studied in Part III).

ACKNOWLEDGMENTS

We are grateful to the EU for a Marie-Curie Postdoctoral Fellowship (SF), to the BBSRC for support (EVB), and to Dr. Martin Baron for 400 MHz NMR access.

REFERENCES

1. Bathini, Y.; Rao, K.E.; Shea, R.G.; Lown, J.W. Chem. Res. Toxicol. **1990**, *3*, 268–80.
2. Ebrahimi, S.E.S.; Bibby, M.C.; Fox, K.R.; Douglas, K.T. Anti-Cancer Drug Design **1995**, *10*, 463–79.
3. Parkinson, J.P.; Sadat-Ebrahimi, S.; Wilton, A.; McKie, J.H.; Andrews, J.; Douglas, K.T. Biochemistry **1995**, *34*, 16240–44.
4. Parkinson, J.A.; Ebrahimi, S.E.; McKie, J.H.; Douglas, K.T. Biochemistry **1994**, *33*, 8442–52.
5. Pasternack, R.F.; Gibbs, E.J.; Villafranca, J.J. Biochemistry **1983**, *22*, 2406–14.
6. Lipscomb, L.A.; Zhou, F.X.; Presnell, S.R.; Woo, R.J.; Peek, M.E.; Plaskon, R.R.; Williams, L.D. Biochemistry **1996**, *35*, 2818–23.
7. Sehlstedt, U.; Kim, S.K.; Carter, P.; Goodisman, J.; Vollano, J.F.; Norden, B.; Dabrowiak, J.C. Biochemistry **1994**, *33*, 417–26.
8. Marzilli, L.G. New. J. Chem. **1990**, *14*, 409–20.
9. Ward, B.; Skorobogaty, A.; Dabrowiak, J.C. Biochemistry **1986**, *25*, 6875–83.
10. Ford, K.; Fox, K.R.; Neidle, S.; Waring, M.J. Nucl. Acids. Res. **1987**, *15*, 2221–34.

MARCEL DEKKER, INC.
270 Madison Avenue, New York, New York 10016

11. Marzilli, L.G.; Banville, D.L.; Zon, G.; Wilson, W.D. J. Amer. Chem. Soc. **1986**, *108*, 4188–92.
12. Bernadou, J.; Pratviel, G.; Bennis, F.; Girardet, M.; Meunier, B. Biochemistry **1989**, *28*, 7268–75.
13. Frau, S.; Bernadou, J.; Meunier, B. Bioconjugate Chem. **1997**, *8*, 222–31.
14. Frau, S.; Bernadou, J; Meunier, B. New J. Chem. **1995**, *19*, 873–76.
15. Bigey, P.; Frau, S.; Loup, C.; Claparols, C.; Bernadou, J.; Meunier, B. Bull. Soc. Chim. Fr. **1996**, *133*, 679–89.
16. Pasternack, R.F.; Garrity, P.; Ehrlich, B.; Davis, C.B.; Gibbs, E.J.; Orloff, G.; Giartosio, A.; Turano, C. Nucl. Acids Res. **1986**, *14*, 5919–31.
17. Bichenkova, E.V.; Marks, D.S.; Lokhov, S.G.; Dobrikov, M.I.; Vlassov, V.V.; Douglas, K.T. J. Biomol. Struct. Dynam. **1997**, *15*, 307–20.
18. McGhee, J.D.; Von Hippel, P.H.J. Mol. Biol. **1974**, *86*, 469–89.
19. Quintana, J.R.; Lipanov, A.A.; Dickerson, R.E. Biochemistry **1991**, *30*, 10294–306.
20. Teng, M.-K.; Usman, N.; Frederick, C.A; Wang, A.H.-J. Nucl. Acids Res. **1988**, *16*, 2671–90.
21. Loontiens, F.G.; Regenfuss, P.; Zechal, A.; Dumortier, L.; Clegg, R.M. Biochemistry **1990**, *29*, 9029–39.
22. Parkinson, J.A.; Barber, J.; Douglas, K.T.; Rosamund, J.; Sharples, D. Biochemistry **1990**, *29*, 10181–90.
23. Sari, M.A.; Battioni, J.P.; Dupre, D.; Mansuy, D.; Le Pecq, J.B. Biochemistry **1990**, *29*, 4205–15.
24. Ward, B.; Skorobogaty, A.; Dabrowiak, J.C. Biochemistry **1986**, *25*, 7827–33.
25. Feng, Y.; Pilbrow, J.R. Biophysical Chemistry **1990**, *36*, 117–31.
26. Pasternack, R.F.; Gurrieri, S.; Lauceri, R.; Purrello, R. Inorg. Chim. Acta **1996**, *246*, 7–12.
27. Fiel, R.J.; Howard, J.C.; Mark, E.H.; Datta Gupta, N. Nucl. Acids Res. **1979**, *6*, 3093–3118.
28. Pasternack, R.F.; Gibbs, E.J.; Villafranca, J.J. Biochemistry **1983**, *22*, 5409–5417.
29. Strickland, J.A.; Marzilli, L.G.; Gay, K.M.; Wilson, W.D. Biochemistry **1988**, *27*, 8870–8878.

Received March 3, 2000
Accepted September 29, 2000

MARCEL DEKKER, INC.
270 Madison Avenue, New York, New York 10016

Request Permission or Order Reprints Instantly!